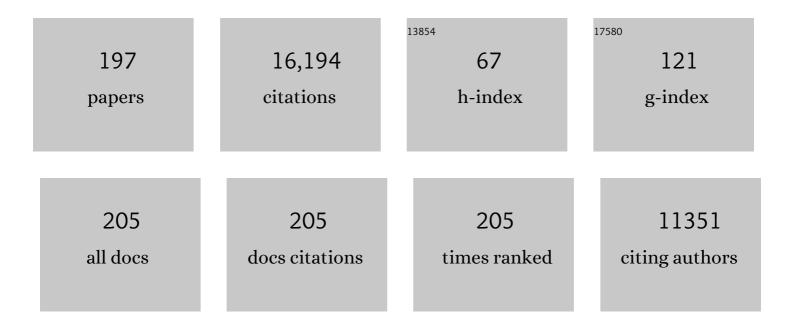
## **Trevor Douglas**

List of Publications by Year in descending order

Source: https://exaly.com/author-pdf/6167473/publications.pdf Version: 2024-02-01



#	Article	IF	CITATIONS
1	Nano-Particulate Platforms for Vaccine Delivery to Enhance Antigen-Specific CD8+ T-Cell Response. Methods in Molecular Biology, 2022, 2412, 367-398.	0.4	0
2	Bioinspired Approaches to Self-Assembly of Virus-like Particles: From Molecules to Materials. Accounts of Chemical Research, 2022, 55, 1349-1359.	7.6	21
3	Multilayered Ordered Protein Arrays Self-Assembled from a Mixed Population of Virus-like Particles. ACS Nano, 2022, 16, 7662-7673.	7.3	8
4	Electromechanical Photophysics of GFP Packed Inside Viral Protein Cages Probed by Forceâ€Fluorescence Hybrid Singleâ€Molecule Microscopy. Small, 2022, 18, .	5.2	7
5	Protein nanocage architectures for the delivery of therapeutic proteins. Current Opinion in Colloid and Interface Science, 2021, 51, 101395.	3.4	19
6	Fluctuating nonlinear spring theory: Strength, deformability, and toughness of biological nanoparticles from theoretical reconstruction of force-deformation spectra. Acta Biomaterialia, 2021, 122, 263-277.	4.1	5
7	Polymer Coatings on Virus-like Particle Nanoreactors at Low Ionic Strength—Charge Reversal and Substrate Access. Biomacromolecules, 2021, 22, 2107-2118.	2.6	14
8	Molecular exclusion limits for diffusion across a porous capsid. Nature Communications, 2021, 12, 2903.	5.8	29
9	Substrate Partitioning into Protein Macromolecular Frameworks for Enhanced Catalytic Turnover. ACS Nano, 2021, 15, 15687-15699.	7.3	19
10	Cytochrome <i>C</i> with peroxidase-like activity encapsulated inside the small DPS protein nanocage. Journal of Materials Chemistry B, 2021, 9, 3168-3179.	2.9	9
11	Controlled Modular Multivalent Presentation of the CD40 Ligand on P22 Virus-like Particles Leads to Tunable Amplification of CD40 Signaling. ACS Applied Bio Materials, 2021, 4, 8205-8214.	2.3	10
12	Tuning the catalytic properties of P22 nanoreactors through compositional control. Nanoscale, 2020, 12, 336-346.	2.8	37
13	Synthetic Virus-like Particles for Glutathione Biosynthesis. ACS Synthetic Biology, 2020, 9, 3298-3310.	1.9	40
14	A Self-Adjuvanted, Modular, Antigenic VLP for Rapid Response to Influenza Virus Variability. ACS Applied Materials & Interfaces, 2020, 12, 18211-18224.	4.0	38
15	Virus-Like Particles (VLPs) as a Platform for Hierarchical Compartmentalization. Biomacromolecules, 2020, 21, 2060-2072.	2.6	26
16	Loading the dice: The orientation of virus-like particles adsorbed on titanate assisted organosilanized surfaces. Biointerphases, 2019, 14, 011001.	0.6	9
17	Virus capsid assembly across different length scales inspire the development of virus-based biomaterials. Current Opinion in Virology, 2019, 36, 38-46.	2.6	25
18	Linker-Mediated Assembly of Virus-Like Particles into Ordered Arrays via Electrostatic Control. ACS Applied Bio Materials, 2019, 2, 2192-2201.	2.3	21

#	Article	IF	CITATIONS
19	Chemically Induced Morphogenesis of P22 Virus-like Particles by the Surfactant Sodium Dodecyl Sulfate. Biomacromolecules, 2019, 20, 389-400.	2.6	13
20	The archaeal Dps nanocage targets kidney proximal tubules via glomerular filtration. Journal of Clinical Investigation, 2019, 129, 3941-3951.	3.9	29
21	Protein cage assembly across multiple length scales. Chemical Society Reviews, 2018, 47, 3433-3469.	18.7	138
22	Stimuli Responsive Hierarchical Assembly of P22 Virus-like Particles. Chemistry of Materials, 2018, 30, 2262-2273.	3.2	17
23	Changes in the stability and biomechanics of P22 bacteriophage capsid during maturation. Biochimica Et Biophysica Acta - General Subjects, 2018, 1862, 1492-1504.	1.1	14
24	Templated Assembly of a Functional Ordered Protein Macromolecular Framework from P22 Virus-like Particles. ACS Nano, 2018, 12, 3541-3550.	7.3	52
25	Modular Self-Assembly of Protein Cage Lattices for Multistep Catalysis. ACS Nano, 2018, 12, 942-953.	7.3	86
26	Cargo Retention inside P22 Virus-Like Particles. Biomacromolecules, 2018, 19, 3738-3746.	2.6	30
27	In Vivo Packaging of Protein Cargo Inside of Virus-Like Particle P22. Methods in Molecular Biology, 2018, 1776, 295-302.	0.4	8
28	Atomic force microscopy of virus shells. Biochemical Society Transactions, 2017, 45, 499-511.	1.6	25
29	Sortase-Mediated Ligation as a Modular Approach for the Covalent Attachment of Proteins to the Exterior of the Bacteriophage P22 Virus-like Particle. Bioconjugate Chemistry, 2017, 28, 2114-2124.	1.8	35
30	Biomedical and Catalytic Opportunities of Virus-Like Particles in Nanotechnology. Advances in Virus Research, 2017, 97, 1-60.	0.9	82
31	Induction of Antiviral Immune Response through Recognition of the Repeating Subunit Pattern of Viral Capsids Is Toll-Like Receptor 2 Dependent. MBio, 2017, 8, .	1.8	31
32	Modular interior loading and exterior decoration of a virus-like particle. Nanoscale, 2017, 9, 10420-10430.	2.8	54
33	RGD targeting of human ferritin iron oxide nanoparticles enhances in vivo MRI of vascular inflammation and angiogenesis in experimental carotid disease and abdominal aortic aneurysm. Journal of Magnetic Resonance Imaging, 2017, 45, 1144-1153.	1.9	40
34	Correlative Lightâ€Electron Microscopy Shows RGDâ€Targeted ZnO Nanoparticles Dissolve in the Intracellular Environment of Triple Negative Breast Cancer Cells and Cause Apoptosis with Intratumor Heterogeneity. Advanced Healthcare Materials, 2016, 5, 1310-1325.	3.9	48
35	Cargo–shell and cargo–cargo couplings govern the mechanics of artificially loaded virus-derived cages. Nanoscale, 2016, 8, 9328-9336.	2.8	60
36	Co-localization of catalysts within a protein cage leads to efficient photochemical NADH and/or hydrogen production. Journal of Materials Chemistry B, 2016, 4, 5375-5384.	2.9	21

#	Article	IF	CITATIONS
37	Tuning Viral Capsid Nanoparticle Stability with Symmetrical Morphogenesis. ACS Nano, 2016, 10, 8465-8473.	7.3	34
38	Targeted Cancer Therapy: Correlative Lightâ€Electron Microscopy Shows RGDâ€Targeted ZnO Nanoparticles Dissolve in the Intracellular Environment of Triple Negative Breast Cancer Cells and Cause Apoptosis with Intratumor Heterogeneity (Adv. Healthcare Mater. 11/2016). Advanced Healthcare Materials, 2016, 5, 1248-1248.	3.9	2
39	Virus Matryoshka: A Bacteriophage Particle—Guided Molecular Assembly Approach to a Monodisperse Model of the Immature Human Immunodeficiency Virus. Small, 2016, 12, 5862-5872.	5.2	8
40	Viruslike Particles Encapsidating Respiratory Syncytial Virus M and M2 Proteins Induce Robust T Cell Responses. ACS Biomaterials Science and Engineering, 2016, 2, 2324-2332.	2.6	50
41	Two-Dimensional Crystallization of P22 Virus-Like Particles. Journal of Physical Chemistry B, 2016, 120, 5938-5944.	1.2	13
42	Programmed Self-Assembly of an Active P22-Cas9 Nanocarrier System. Molecular Pharmaceutics, 2016, 13, 1191-1196.	2.3	73
43	Self-assembling biomolecular catalysts for hydrogen production. Nature Chemistry, 2016, 8, 179-185.	6.6	170
44	Tailored delivery of analgesic ziconotide across a blood brain barrier model using viral nanocontainers. Scientific Reports, 2015, 5, 12497.	1.6	56
45	Developing a Dissociative Nanocontainer for Peptide Drug Delivery. International Journal of Environmental Research and Public Health, 2015, 12, 12543-12555.	1.2	19
46	Design of a VLP-nanovehicle for CYP450 enzymatic activity delivery. Journal of Nanobiotechnology, 2015, 13, 66.	4.2	67
47	Symmetry Controlled, Genetic Presentation of Bioactive Proteins on the P22 Virus-like Particle Using an External Decoration Protein. ACS Nano, 2015, 9, 9134-9147.	7.3	66
48	Hybrid Nanoreactors: Coupling Enzymes and Smallâ€Molecule Catalysts within Virusâ€Like Particles. Israel Journal of Chemistry, 2015, 55, 96-101.	1.0	19
49	Selective Biotemplated Synthesis of TiO <sub>2</sub> Inside a Protein Cage. Biomacromolecules, 2015, 16, 214-218.	2.6	26
50	Higher Order Assembly of Virusâ€like Particles (VLPs) Mediated by Multiâ€valent Protein Linkers. Small, 2015, 11, 1562-1570.	5.2	36
51	Gadolinium-Loaded Viral Capsids as Magnetic Resonance Imaging Contrast Agents. Applied Magnetic Resonance, 2015, 46, 349-355.	0.6	20
52	Development of virusâ€like particles for diagnostic and prophylactic biomedical applications. Wiley Interdisciplinary Reviews: Nanomedicine and Nanobiotechnology, 2015, 7, 722-735.	3.3	65
53	Interligand Electron Transfer in Heteroleptic Ruthenium(II) Complexes Occurs on Multiple Time Scales. Journal of Physical Chemistry A, 2015, 119, 4813-4824.	1.1	36
54	Use of Protein Cages as a Template for Confined Synthesis of Inorganic and Organic Nanoparticles. Methods in Molecular Biology, 2015, 1252, 17-25.	0.4	13

#	Article	IF	CITATIONS
55	Manganese(III) porphyrins complexed with P22 virus-like particles as T 1-enhanced contrast agents for magnetic resonance imaging. Journal of Biological Inorganic Chemistry, 2014, 19, 237-246.	1.1	22
56	CD11c + cells primed with unrelated antigens facilitate an accelerated immune response to influenza virus in mice. European Journal of Immunology, 2014, 44, 397-408.	1.6	11
57	Constructing catalytic antimicrobial nanoparticles by encapsulation of hydrogen peroxide producing enzyme inside the P22 VLP. Journal of Materials Chemistry B, 2014, 2, 5948.	2.9	36
58	X-ray spatial frequency heterodyne imaging of protein-based nanobubble contrast agents. Optics Express, 2014, 22, 23290.	1.7	8
59	Encapsulation of an Enzyme Cascade within the Bacteriophage P22 Virus-Like Particle. ACS Chemical Biology, 2014, 9, 359-365.	1.6	213
60	Rescuing recombinant proteins by sequestration into the P22 VLP. Chemical Communications, 2013, 49, 10412-10414.	2.2	41
61	Stabilizing viral nano-reactors for nerve-agent degradation. Biomaterials Science, 2013, 1, 881.	2.6	29
62	Atom transfer radical polymerization on the interior of the P22 capsid and incorporation of photocatalytic monomer crosslinks. European Polymer Journal, 2013, 49, 2976-2985.	2.6	23
63	Biomimetic Antigenic Nanoparticles Elicit Controlled Protective Immune Response to Influenza. ACS Nano, 2013, 7, 3036-3044.	7.3	98
64	Unravelling capsid transformations. Nature Chemistry, 2013, 5, 444-445.	6.6	5
65	P22 Viral Capsids as Nanocomposite High-Relaxivity MRI Contrast Agents. Molecular Pharmaceutics, 2013, 10, 11-17.	2.3	69
66	Location of the Bacteriophage P22 Coat Protein C-Terminus Provides Opportunities for the Design of Capsid-Based Materials. Biomacromolecules, 2013, 14, 2989-2995.	2.6	41
67	Inducible Bronchus-Associated Lymphoid Tissue (iBALT) Synergizes with Local Lymph Nodes during Antiviral CD4 <sup>+</sup> T Cell Responses. Lymphatic Research and Biology, 2013, 11, 196-202.	0.5	26
68	Topological Biosignatures: Large-Scale Structure of Chemical Networks from Biology and Astrochemistry. Astrobiology, 2012, 12, 29-39.	1.5	15
69	Characterization of the Bacteroides fragilis bfr Gene Product Identifies a Bacterial DPS-Like Protein and Suggests Evolutionary Links in the Ferritin Superfamily. Journal of Bacteriology, 2012, 194, 15-27.	1.0	20
70	Nanoreactors by Programmed Enzyme Encapsulation Inside the Capsid of the Bacteriophage P22. ACS Nano, 2012, 6, 5000-5009.	7.3	238
71	A virus-like particle vaccine platform elicits heightened and hastened local lung mucosal antibody production after a single dose. Vaccine, 2012, 30, 3653-3665.	1.7	31
72	Use of the interior cavity of the P22 capsid for site-specific initiation of atom-transfer radical polymerization with high-density cargo loading. Nature Chemistry, 2012, 4, 781-788.	6.6	163

#	Article	IF	CITATIONS
73	Virus-Like Particle-Induced Protection Against MRSA Pneumonia Is Dependent on IL-13 and Enhancement of Phagocyte Function. American Journal of Pathology, 2012, 181, 196-210.	1.9	28
74	Proteomic Analysis of <i>Sulfolobus solfataricus</i> during <i>Sulfolobus</i> Turreted Icosahedral Virus Infection. Journal of Proteome Research, 2012, 11, 1420-1432.	1.8	26
75	Virus-like particle nanoreactors: programmed encapsulation of the thermostable CelB glycosidase inside the P22 capsid. Soft Matter, 2012, 8, 10158.	1.2	100
76	Coconfinement of Fluorescent Proteins: Spatially Enforced Communication of GFP and mCherry Encapsulated within the P22 Capsid. Biomacromolecules, 2012, 13, 3902-3907.	2.6	71
77	Site-Directed Coordination Chemistry with P22 Virus-like Particles. Langmuir, 2012, 28, 1998-2006.	1.6	38
78	RGD-Conjugated Human Ferritin Nanoparticles for Imaging Vascular Inflammation and Angiogenesis in Experimental Carotid and Aortic Disease. Molecular Imaging and Biology, 2012, 14, 315-324.	1.3	64
79	Photo-induced H2 production by [NiFe]-hydrogenase from T. roseopersicina covalently linked to a Ru(II) photosensitizer. Journal of Inorganic Biochemistry, 2012, 106, 151-155.	1.5	38
80	Protein Cage Nanoparticles Bearing the LyP-1 Peptide for Enhanced Imaging of Macrophage-Rich Vascular Lesions. ACS Nano, 2011, 5, 2493-2502.	7.3	98
81	Templated assembly of organic–inorganic materials using the core shell structure of the P22 bacteriophage. Chemical Communications, 2011, 47, 6326.	2.2	44
82	Structure and photoelectrochemistry of a virus capsid–TiO2nanocomposite. Nanoscale, 2011, 3, 1004-1007.	2.8	27
83	Monitoring Structural Transitions in Icosahedral Virus Protein Cages by Site-Directed Spin Labeling. Journal of the American Chemical Society, 2011, 133, 4156-4159.	6.6	11
84	All in the Packaging: Structural and Electronic Effects of Nanoconfinement on Metal Oxide Nanoparticles. Chemistry of Materials, 2011, 23, 3921-3929.	3.2	6
85	Biomimetic FePt nanoparticle synthesis within Pyrococcus furiosus ferritins and their layer-by-layer formation. Soft Matter, 2011, 7, 11078.	1.2	24
86	Structure, dynamics, and solvation in a disordered metal–organic coordination polymer: a multiscale study. Journal of Coordination Chemistry, 2011, 64, 4301-4317.	0.8	5
87	Genetically Programmed In Vivo Packaging of Protein Cargo and Its Controlled Release from Bacteriophage P22. Angewandte Chemie - International Edition, 2011, 50, 7425-7428.	7.2	147
88	Human ferritin cages for imaging vascular macrophages. Biomaterials, 2011, 32, 1430-1437.	5.7	105
89	A NETWORK-THEORETICAL APPROACH TO UNDERSTANDING INTERSTELLAR CHEMISTRY. Astrophysical Journal, 2010, 722, 1921-1931.	1.6	8
90	Protein cage nanoparticles as secondary building units for the synthesis of 3-dimensional coordination polymers. Soft Matter, 2010, 6, 3167.	1.2	27

#	Article	IF	CITATIONS
91	Biomimetic synthesis of photoactive α-Fe <sub>2</sub> O <sub>3</sub> templated by the hyperthermophilic ferritin from Pyrococus furiosus. Journal of Materials Chemistry, 2010, 20, 65-67.	6.7	21
92	Targeted Delivery of a Photosensitizer to <i>Aggregatibacter actinomycetemcomitans</i> Biofilm. Antimicrobial Agents and Chemotherapy, 2010, 54, 2489-2496.	1.4	30
93	Some Enzymes Just Need a Space of Their Own. Science, 2010, 327, 42-43.	6.0	31
94	Two-component magnetic structure of iron oxide nanoparticles mineralized in <i>Listeria innocua</i> protein cages. Journal of Applied Physics, 2010, 107, .	1.1	13
95	Swelling and Softening of the CCMV Plant Virus Capsid in Response toÂpH Shifts. Biophysical Journal, 2010, 98, 656a.	0.2	4
96	Hydrogen Enhances Nickel Tolerance in the Purple Sulfur Bacterium Thiocapsa roseopersicina. Environmental Science & Technology, 2010, 44, 834-840.	4.6	9
97	Ion Accumulation in a Protein Nanocage: Finding Noisy Temporal Sequences Using a Genetic Algorithm. Biophysical Journal, 2010, 99, 3385-3393.	0.2	6
98	Size and Crystallinity in Protein-Templated Inorganic Nanoparticles. Chemistry of Materials, 2010, 22, 4612-4618.	3.2	37
99	Implementation of P22 Viral Capsids as Nanoplatforms. Biomacromolecules, 2010, 11, 2804-2809.	2.6	87
100	The ferritin superfamily: Supramolecular templates for materials synthesis. Biochimica Et Biophysica Acta - General Subjects, 2010, 1800, 834-845.	1.1	210
101	A click chemistry based coordination polymer inside small heat shock protein. Chemical Communications, 2010, 46, 264-266.	2.2	40
102	Virus particles as active nanomaterials that can rapidly change their viscoelastic properties in response to dilute solutions. Soft Matter, 2010, 6, 5286.	1.2	12
103	Something Old, Something New, Something Borrowed; How the Thermoacidophilic Archaeon Sulfolobus solfataricus Responds to Oxidative Stress. PLoS ONE, 2009, 4, e6964.	1.1	70
104	Inducible Bronchus-Associated Lymphoid Tissue Elicited by a Protein Cage Nanoparticle Enhances Protection in Mice against Diverse Respiratory Viruses. PLoS ONE, 2009, 4, e7142.	1.1	113
105	Structural and Functional Studies of Archaeal Viruses. Journal of Biological Chemistry, 2009, 284, 12599-12603.	1.6	96
106	Supramolecular Protein Cage Composite MR Contrast Agents with Extremely Efficient Relaxivity Properties. Nano Letters, 2009, 9, 4520-4526.	4.5	59
107	Particle Assembly and Ultrastructural Features Associated with Replication of the Lytic Archaeal Virus <i>Sulfolobus</i> Turreted Icosahedral Virus. Journal of Virology, 2009, 83, 5964-5970.	1.5	96
108	Intracellular Distribution of Macrophage Targeting Ferritin–Iron Oxide Nanocomposite. Advanced Materials, 2009, 21, 458-462.	11.1	48

#	Article	IF	CITATIONS
109	Correct charge state assignment of native electrospray spectra of protein complexes. Journal of the American Society for Mass Spectrometry, 2009, 20, 435-442.	1.2	23
110	Determination of anisotropy constants of protein encapsulated iron oxide nanoparticles by electron magnetic resonance. Journal of Magnetism and Magnetic Materials, 2009, 321, 175-180.	1.0	29
111	Janus-like Protein Cages. Spatially Controlled Dual-Functional Surface Modifications of Protein Cages. Nano Letters, 2009, 9, 2360-2366.	4.5	47
112	Synthesis of a Cross-Linked Branched Polymer Network in the Interior of a Protein Cage. Journal of the American Chemical Society, 2009, 131, 4346-4354.	6.6	77
113	Synergistic Effects of Mutations and Nanoparticle Templating in the Self-Assembly of Cowpea Chlorotic Mottle Virus Capsids. Nano Letters, 2009, 9, 393-398.	4.5	57
114	A Streptavidinâ^'Protein Cage Janus Particle for Polarized Targeting and Modular Functionalization. Journal of the American Chemical Society, 2009, 131, 9164-9165.	6.6	63
115	In-Plane Ordering of a Genetically Engineered Viral Protein Cage. Journal of Adhesion, 2009, 85, 69-77.	1.8	4
116	Genetics, biochemistry and structure of the archaeal virus STIV. Biochemical Society Transactions, 2009, 37, 114-117.	1.6	14
117	A human ferritin iron oxide nanoâ€composite magnetic resonance contrast agent. Magnetic Resonance in Medicine, 2008, 60, 1073-1081.	1.9	134
118	Monitoring Biomimetic Platinum Nanocluster Formation Using Mass Spectrometry and Clusterâ€Dependent H <sub>2</sub> Production. Angewandte Chemie - International Edition, 2008, 47, 7845-7848.	7.2	40
119	Biomimetic synthesis of β-TiO2 inside a viral capsid. Journal of Materials Chemistry, 2008, 18, 3821.	6.7	75
120	Plant Viruses as Biotemplates for Materials and Their Use in Nanotechnology. Annual Review of Phytopathology, 2008, 46, 361-384.	3.5	233
121	Signal ampflication using nanoplatform cluster formation. Soft Matter, 2008, 4, 2519.	1.2	10
122	Photochemical Mineralization of Europium, Titanium, and Iron Oxyhydroxide Nanoparticles in the Ferritin Protein Cage. Inorganic Chemistry, 2008, 47, 2237-2239.	1.9	85
123	Expanding the Temperature Range of Biomimetic Synthesis Using a Ferritin from the Hyperthermophile <i>Pyrococcus furiosus</i> . Chemistry of Materials, 2008, 20, 1541-1547.	3.2	32
124	Controlled Assembly of Bifunctional Chimeric Protein Cages and Composition Analysis Using Noncovalent Mass Spectrometry. Journal of the American Chemical Society, 2008, 130, 16527-16529.	6.6	69
125	Transcriptome Analysis of Infection of the Archaeon <i>Sulfolobus solfataricus</i> with <i>Sulfolobus</i> Turreted Icosahedral Virus. Journal of Virology, 2008, 82, 4874-4883.	1.5	84
126	Biomimetic Synthesis of an Active H2 Catalyst Using the Ferritin Protein Cage Architecture. ACS Symposium Series, 2008, , 263-272.	0.5	1

#	Article	IF	CITATIONS
127	Virus movement maintains local virus population diversity. Proceedings of the National Academy of Sciences of the United States of America, 2007, 104, 19102-19107.	3.3	70
128	Bioprospecting in high temperature environments; application of thermostable protein cages. Soft Matter, 2007, 3, 1091.	1.2	11
129	Synthetic Control over Magnetic Moment and Exchange Bias in All-Oxide Materials Encapsulated within a Spherical Protein Cage. Journal of the American Chemical Society, 2007, 129, 197-201.	6.6	91
130	Biological Containers: Protein Cages as Multifunctional Nanoplatforms. Advanced Materials, 2007, 19, 1025-1042.	11.1	518
131	Viral capsids as MRI contrast agents. Magnetic Resonance in Medicine, 2007, 58, 871-879.	1.9	120
132	High-Density Targeting of a Viral Multifunctional Nanoplatform to a Pathogenic, Biofilm-Forming Bacterium. Chemistry and Biology, 2007, 14, 387-398.	6.2	58
133	Targeting and Photodynamic Killing of a Microbial Pathogen Using Protein Cage Architectures Functionalized with a Photosensitizer. Langmuir, 2007, 23, 12280-12286.	1.6	97
134	Biodistribution studies of protein cage nanoparticles demonstrate broad tissue distribution and rapid clearance in vivo. International Journal of Nanomedicine, 2007, 2, 715-33.	3.3	111
135	Targeting of Cancer Cells with Ferrimagnetic Ferritin Cage Nanoparticles. Journal of the American Chemical Society, 2006, 128, 16626-16633.	6.6	359
136	Assembly of Multilayer Films Incorporating a Viral Protein Cage Architecture. Langmuir, 2006, 22, 8891-8896.	1.6	66
137	Viruses: Making Friends with Old Foes. Science, 2006, 312, 873-875.	6.0	568
138	Structure of the DPS-Like Protein fromSulfolobus solfataricusReveals a Bacterioferritin-Like Dimetal Binding Site within a DPS-Like Dodecameric Assemblyâ€,‡. Biochemistry, 2006, 45, 10815-10827.	1.2	61
139	A radical solution for the biosynthesis of the H-cluster of hydrogenase. FEBS Letters, 2006, 580, 363-367.	1.3	72
140	Hot crenarchaeal viruses reveal deep evolutionary connections. Nature Reviews Microbiology, 2006, 4, 520-528.	13.6	59
141	Melanoma and Lymphocyte Cell-Specific Targeting Incorporated into a Heat Shock Protein Cage Architecture. Chemistry and Biology, 2006, 13, 161-170.	6.2	146
142	Dps-like protein from the hyperthermophilic archaeon Pyrococcus furiosus. Journal of Inorganic Biochemistry, 2006, 100, 1061-1068.	1.5	49
143	Characterization of the Archaeal Thermophile Sulfolobus Turreted Icosahedral Virus Validates an Evolutionary Link among Double-Stranded DNA Viruses from All Domains of Life. Journal of Virology, 2006, 80, 7625-7635.	1.5	86
144	Electron magnetic resonance of iron oxide nanoparticles mineralized in protein cages. Journal of Applied Physics, 2005, 97, 10M523.	1.1	17

#	Article	IF	CITATIONS
145	Bio-inspired Synthesis of Protein-Encapsulated CoPt Nanoparticles. Advanced Functional Materials, 2005, 15, 1489-1494.	7.8	136
146	Paramagnetic viral nanoparticles as potential high-relaxivity magnetic resonance contrast agents. Magnetic Resonance in Medicine, 2005, 54, 807-812.	1.9	198
147	Structural transitions in Cowpea chlorotic mottle virus (CCMV). Physical Biology, 2005, 2, S166-S172.	0.8	54
148	From The Cover: An archaeal antioxidant: Characterization of a Dps-like protein from Sulfolobus solfataricus. Proceedings of the National Academy of Sciences of the United States of America, 2005, 102, 10551-10556.	3.3	114
149	Biomimetic Synthesis of a H2 Catalyst Using a Protein Cage Architecture. Nano Letters, 2005, 5, 2306-2309.	4.5	119
150	Influence of Electrostatic Interactions on the Surface Adsorption of a Viral Protein Cage. Langmuir, 2005, 21, 8686-8693.	1.6	47
151	Immobilization of Active Hydrogenases by Encapsulation in Polymeric Porous Gels. Nano Letters, 2005, 5, 2085-2087.	4.5	21
152	Surface contribution to the anisotropy energy of spherical magnetite particles. Journal of Applied Physics, 2005, 97, 10B301.	1.1	44
153	Modeling of the magnetic behavior of γ-Fe2O3 nanoparticles mineralized in ferritin. Journal of Applied Physics, 2004, 95, 7127-7129.	1.1	29
154	From The Cover: The structure of a thermophilic archaeal virus shows a double-stranded DNA viral capsid type that spans all domains of life. Proceedings of the National Academy of Sciences of the United States of America, 2004, 101, 7716-7720.	3.3	219
155	Comparative Genomic Analysis of Hyperthermophilic Archaeal Fuselloviridae Viruses. Journal of Virology, 2004, 78, 1954-1961.	1.5	131
156	Heterologous expression of the modified coat protein of Cowpea chlorotic mottle bromovirus results in the assembly of protein cages with altered architectures and function. Journal of General Virology, 2004, 85, 1049-1053.	1.3	96
157	Iron and Cobalt Oxide and Metallic Nanoparticles Prepared from Ferritin. Langmuir, 2004, 20, 10283-10287.	1.6	80
158	Charge Development on Ferritin: An Electrokinetic Study of a Protein Containing a Ferrihydrite Nanoparticle. ACS Symposium Series, 2004, , 226-229.	0.5	2
159	Effects of Culturing on the Population Structure of a Hyperthermophilic Virus. Microbial Ecology, 2004, 48, 561-566.	1.4	22
160	Microbe Manufacturers of Semiconductors. Chemistry and Biology, 2004, 11, 1478-1480.	6.2	16
161	Photocatalytic Synthesis of Copper Colloids from Cu(II) by the Ferrihydrite Core of Ferritin. Inorganic Chemistry, 2004, 43, 3441-3446.	1.9	79
162	Preparation of Magnetically Labeled Cells for Cell Tracking by Magnetic Resonance Imaging. Methods in Enzymology, 2004, 386, 275-299.	0.4	164

#	Article	IF	CITATIONS
163	A Bioengineering Approach to the Production of Metal and Metal Oxide Nanoparticles. ACS Symposium Series, 2004, , 230-237.	0.5	0
164	Metal binding to cowpea chlorotic mottle virus using terbium(III) fluorescence. Journal of Biological Inorganic Chemistry, 2003, 8, 721-725.	1.1	52
165	2-D Array Formation of Genetically Engineered Viral Cages on Au Surfaces and Imaging by Atomic Force Microscopy. Journal of the American Chemical Society, 2003, 125, 10806-10807.	6.6	106
166	The Small Heat Shock Protein Cage from Methanococcus jannaschii Is a Versatile Nanoscale Platform for Genetic and Chemical Modification. Nano Letters, 2003, 3, 1573-1576.	4.5	165
167	Constrained Synthesis of Cobalt Oxide Nanomaterials in the 12-Subunit Protein Cage fromListeria innocua. Inorganic Chemistry, 2003, 42, 6300-6305.	1.9	152
168	MATERIALS SCIENCE: A Bright Bio-Inspired Future. Science, 2003, 299, 1192-1193.	6.0	76
169	Protein Engineering of a Viral Cage for Constrained Nanomaterials Synthesis. Advanced Materials, 2002, 14, 415-418.	11.1	365
170	Protein Cage Constrained Synthesis of Ferrimagnetic Iron Oxide Nanoparticles. Advanced Materials, 2002, 14, 1562-1565.	11.1	184
171	Photochemical Reactivity of Ferritin for Cr(VI) Reduction. Chemistry of Materials, 2002, 14, 4874-4879.	3.2	59
172	Synthesis and Characterization of Soluble Iron Oxideâ^'Dendrimer Composites. Chemistry of Materials, 2001, 13, 2201-2209.	3.2	189
173	Ordered association of tobacco mosaic virus in the presence of divalent metal ions. Journal of Inorganic Biochemistry, 2001, 84, 233-240.	1.5	42
174	Magnetodendrimers allow endosomal magnetic labeling and in vivo tracking of stem cells. Nature Biotechnology, 2001, 19, 1141-1147.	9.4	1,016
175	Nanophase Cobalt Oxyhydroxide Mineral Synthesized within the Protein Cage of Ferritin. Inorganic Chemistry, 2000, 39, 1828-1830.	1.9	278
176	Synthesis and characterization of hydrophobic ferritin proteins. Journal of Inorganic Biochemistry, 1999, 76, 187-195.	1.5	52
177	Inorganic-Organic Nanotube Composites from Template Mineralization of Tobacco Mosaic Virus. Advanced Materials, 1999, 11, 253-256.	11.1	698
178	Virus Particles as Templates for Materials Synthesis. Advanced Materials, 1999, 11, 679-681.	11.1	189
179	Inorganic–Organic Nanotube Composites from Template Mineralization of Tobacco Mosaic Virus. , 1999, 11, 253.		3
180	Inorganic–Organic Nanotube Composites from Template Mineralization of Tobacco Mosaic Virus. , 1999, 11, 253.		6

#	Article	IF	CITATIONS
181	Host–guest encapsulation of materials by assembled virus protein cages. Nature, 1998, 393, 152-155.	13.7	887
182	Calculated electrostatic gradients in recombinant human Hâ€chain ferritin. Protein Science, 1998, 7, 1083-1091.	3.1	148
183	Biomimetic Synthesis and Characterization of Magnetic Proteins (Magnetoferritin). Chemistry of Materials, 1998, 10, 279-285.	3.2	204
184	Classical and quantum magnetism in synthetic ferritin proteins. Journal of Applied Physics, 1996, 79, 5324.	1.1	41
185	Reconstitution of manganese oxide cores in horse spleen and recombinant ferritins. Journal of Inorganic Biochemistry, 1995, 58, 59-68.	1.5	187
186	Classical and quantum magnetic phenomena in natural and artificial ferritin proteins. Science, 1995, 268, 77-80.	6.0	236
187	Synthesis and Structure of an Iron(III) Sulfide-Ferritin Bioinorganic Nanocomposite. Science, 1995, 269, 54-57.	6.0	293
188	Initial assessment of magnetoferritin biokinetics and proton relaxation enhancement in rats. Academic Radiology, 1995, 2, 871-878.	1.3	35
189	Persistent oral contrast agent lining the intestine in severe mucosal disease: elucidation of radiographic appearance Radiology, 1994, 191, 747-749.	3.6	8
190	Magnetoferritin: Characterization of a novel superparamagnetic MR contrast agent. Journal of Magnetic Resonance Imaging, 1994, 4, 497-505.	1.9	162
191	Oriented nucleation of gypsum (CaSO4·2H2O) under compressed Langmuir monolayers. Materials Science and Engineering C, 1994, 1, 193-199.	3.8	16
192	Mössbauer spectroscopic and magnetic studies of magnetoferritin. Hyperfine Interactions, 1994, 91, 847-851.	0.2	20
193	Further Characterisation of Forms of Haemosiderin in Iron-Overloaded Tissues. FEBS Journal, 1994, 225, 187-194.	0.2	31
194	Magnetoferritin. Investigative Radiology, 1994, 29, S214-S216.	3.5	40
195	Molecular precursors for indium phosphide and synthesis of small III-V semiconductor clusters in solution. Inorganic Chemistry, 1991, 30, 594-596.	1.9	91
196	A phospholyl complex of indium. Polyhedron, 1990, 9, 329-333.	1.0	14
197	Synthesis and Crystal Structure of a Phospholyl Anion. Angewandte Chemie International Edition in English, 1989, 28, 1367-1368.	4.4	85